Electronic Supplementary Material (ESI) for Journal of Materials Chemistry A.

Supporting Information

N-Carbon coated P-W_2C composite as Efficient Electrocatalyst for Hydrogen Evolution Reaction at All pH Range

Gang Yan, [a†] Caixia Wu, [a†] Huaqiao Tan,* [a] Xiaojia Feng, [b] Likai Yan, * [a] Hongying Zang, [a] Yangguang Li* [a]

Contents

1. Physical characterization of P-W_2C@NC

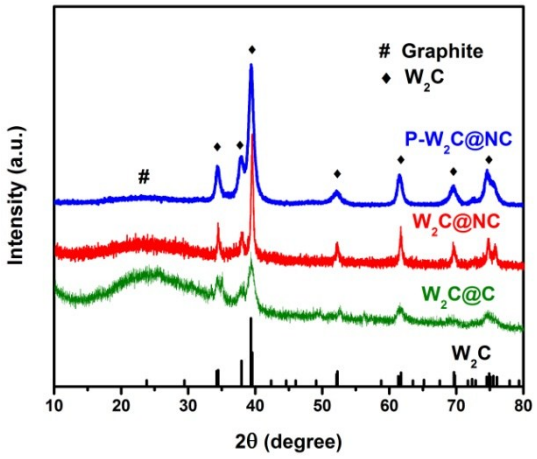

Fig S1. Power XRD patterns of P-W_2C@NC, W_2C@NC and W_2C@C. The result indicated that the pure phase of W_2C was successfully obtained in our method.

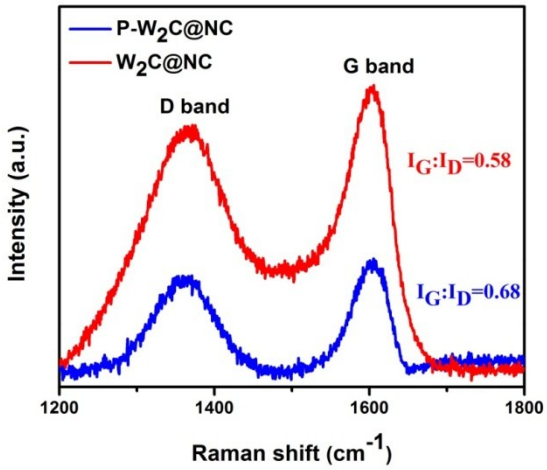

Fig S2. Raman spectral of P-W_2C@NC and W_2C@NC. The I_G/I_D of P-W_2C@NC and W_2C@NC are 0.68 and 0.58, respectively. These results suggest that the graphitization degree of P-W_2C@NC was higher than that of W_2C@NC which can accelerate the charge transfer and enhance the electrocatalytic performance.

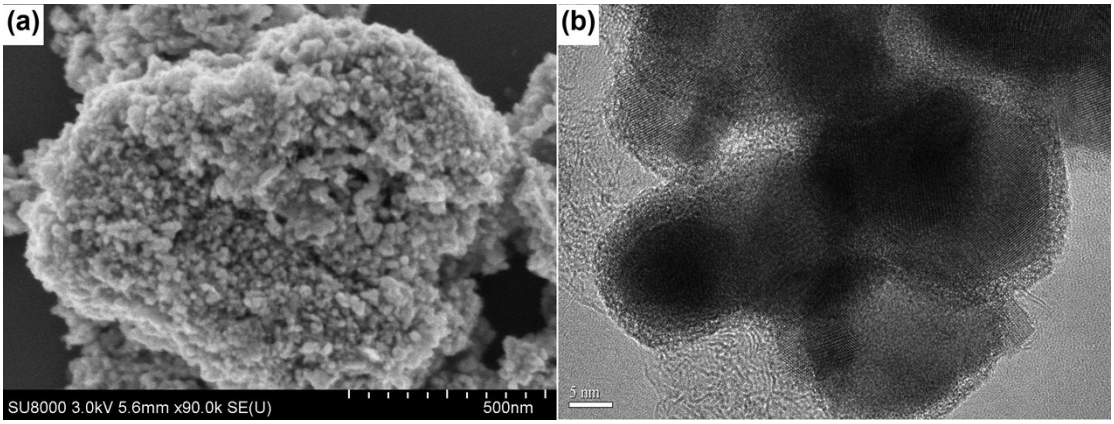

Fig S3. (a) and (b) SEM and HRTEM images of P-W_2C@NC annealed at 800 ^oC for 5 hour under N_2 atmosphere. The image showed that as-synthesizes superstructure P-W_2C@NC was assembled from nano particles. The HRTEM images indicated that the W_2C particles were coated with carbon shells which can protect W_2C from corrosion in basic or neutral solutions.

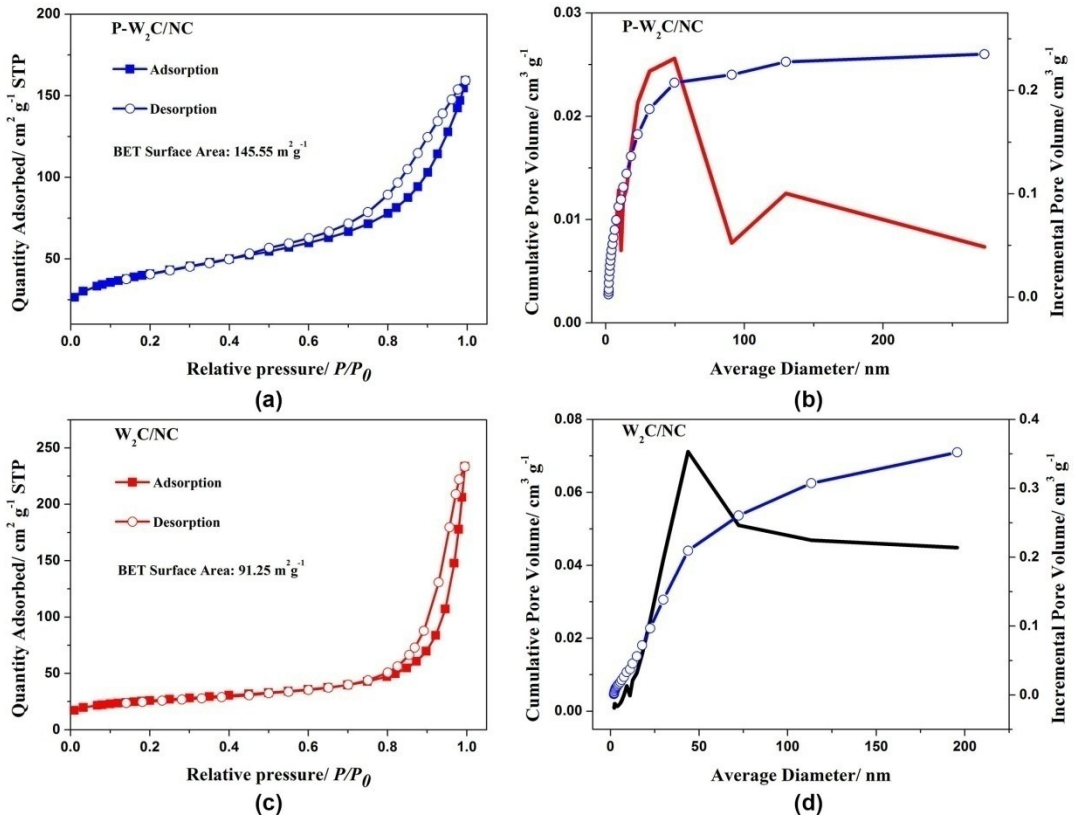

Fig S4. (a and b) The N_2 adsorption-desorption isotherms and the pore-size distribution of P-W_2C@NC and (c and d) W_2C@NC. The BET surface area of P-W_2C@NC (145.55 m^2 g^{-1}) was larger than that of W_2C@NC (91.25 m^2 g^{-1}). The high surface area and the mesoporous structure of P-W_2C@NC may efficiently facilitate electrolyte penetration and charge transfer.

2. Additional electrochemical experiments of P-W_2C@NC

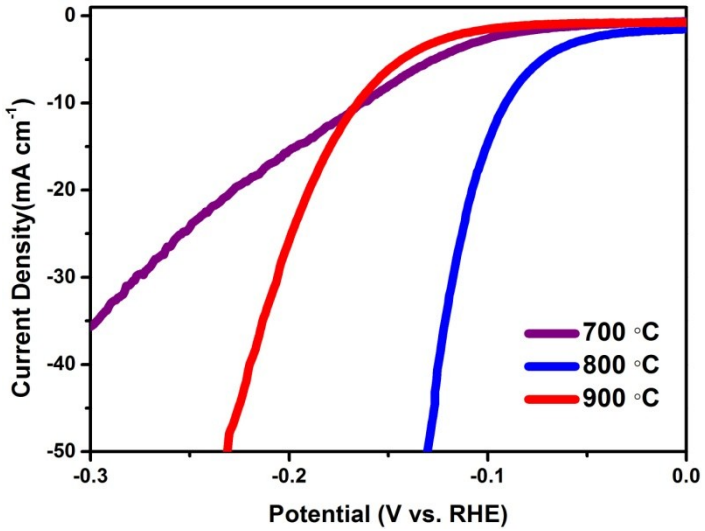

Fig. S5. Comparison of catalytic activities of samples with same mass ratio 1:5 synthesized at different temperature in 0.5 M H_2SO_4. This result showed that the most optimal pyrolysis temperature is 800 ^oC.

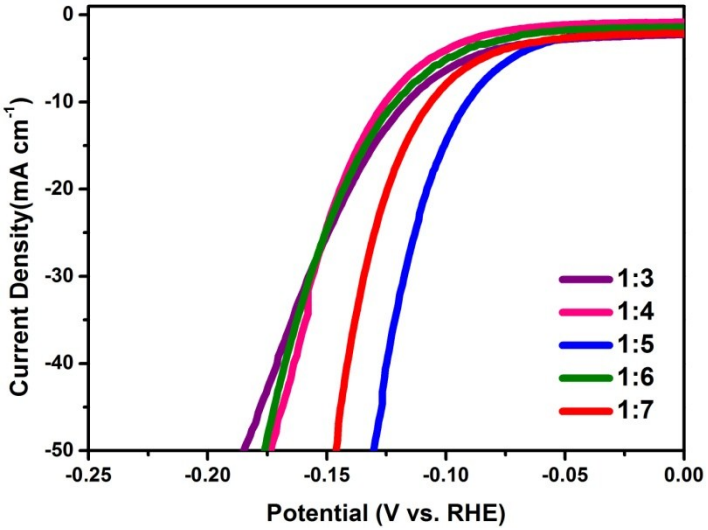

Fig S6. Comparison of catalytic activities of five samples synthesized at different ratios of starting materials in 0.5 M H_2SO_4. The results indicate that the most optimal weight ratio is found to be 1:5.

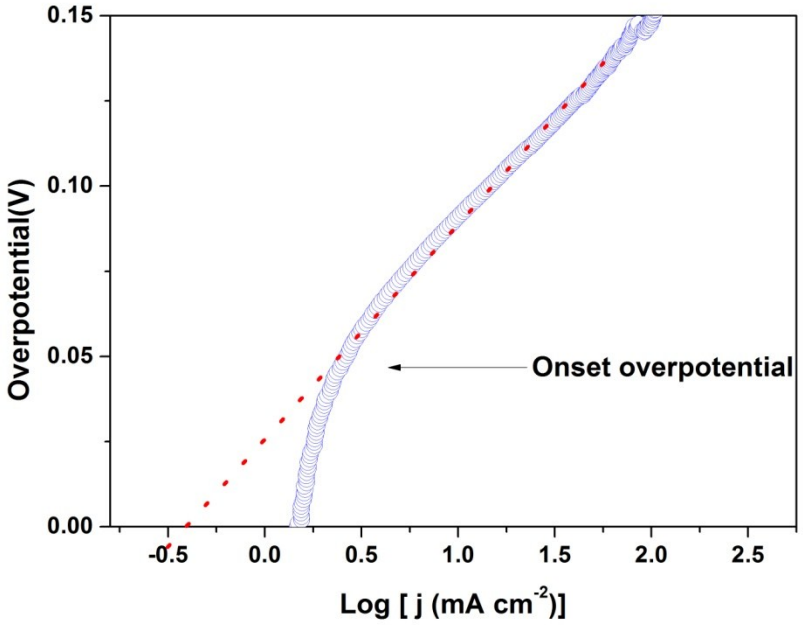

Fig S7. The tafel plot of P-W_2C@NC in the region of low current densities in 0.5 M H_2SO_4. The onset overpotential, as indicated by the arrow, is determined by the potential when the plot starts to deviate from the linear region.

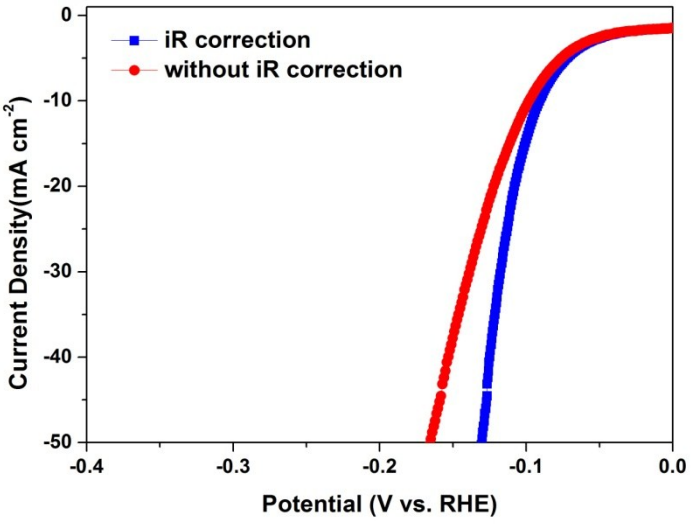

Fig S8. The LSV curves of P-W_2C@NC before and after iR correction.

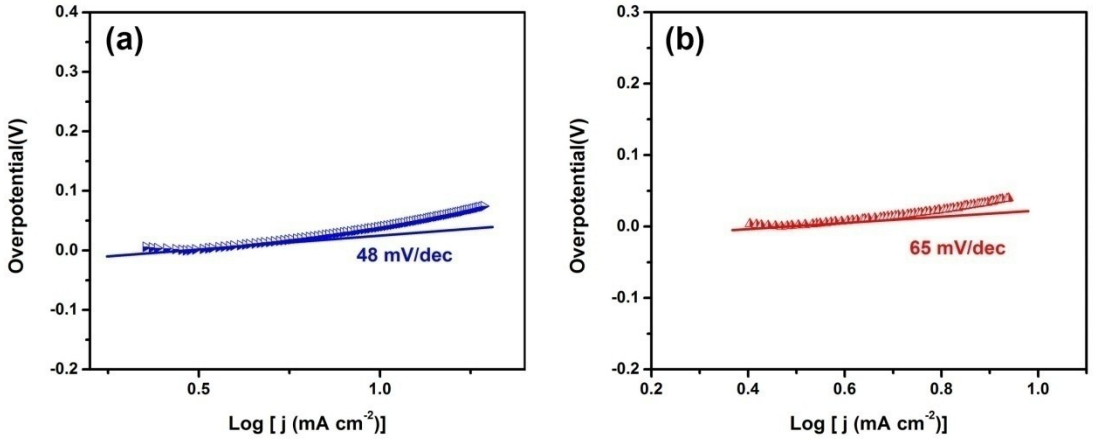

Fig S9. Tafel plots of Pt/C in both (a) alkaline and (b) neutral solutions.

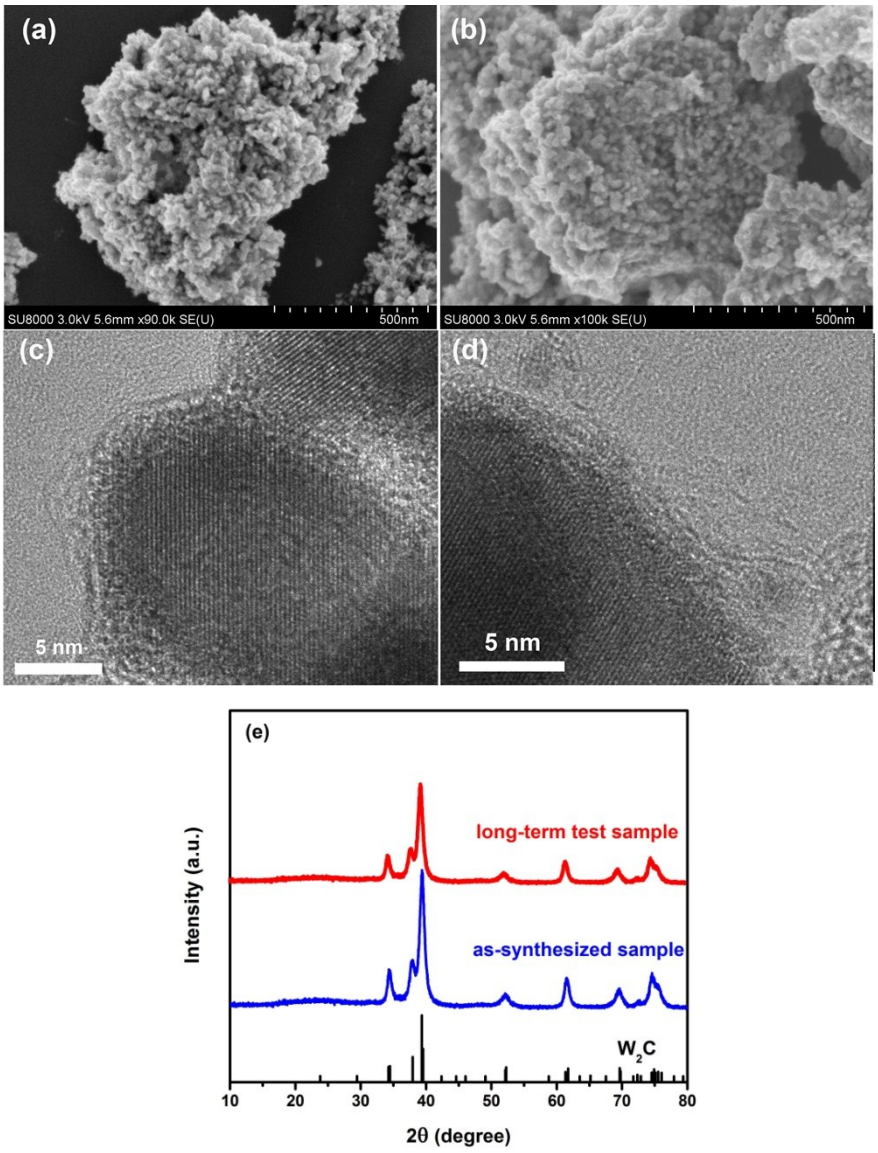

Fig. S10 The SEM images of catalyst (a) before and (b) after long-term test, TEM images of catalyst (c) before and (d) after long-term test, (e) XRD pattern of catalyst

after long-term test. These experiments were carried out at 0.5 M H_2SO_4 solution.

The morphology and structure of catalyst after long-term test have been characterized by SEM, TEM and XRD. As shown in Fig. S10, SEM, TEM, and XRD reveal that negligible change has been observed for the morphology and structure of catalysts after long-term test in acidic media,, which indicates that the catalyst has long-term stability.

3.**List of HER performance in acid, basic and neutral media for reported W_2C@P-NC electrocatalysts**

Table S1. Comparison of HER performance for **P-W_2C@NC** with other tungsten carbide-based electrocatalysts in acid media.

Catalysts	Current density (j, mA cm^{-2})	η at corresponding j (mV)	Tafel slope (mV $decade^{-1}$)	Exchange current density j_0 (mA cm^{-2})	Experimental conditions	Ref.
P-W_2C@NC	**10** **50**	**89** **127**	**53**	**0.316**	**Electrolyte: 0.5 M H_2SO_4; Scan rate: 2 mV s^{-1}**	**This work**
W_2C microsphere	10	~170 (a)	118	0.281	Electrolyte: 1 M H_2SO_4; Scan rate: 5 mV s^{-1}	1
WC-CNTs	10 117.6	145 300	72	~0.1 (c)	Electrolyte: 0.05 M H_2SO_4; Scan rate: 10 mV s^{-1}	2
$WSoy_{0.7}GnP_{10}$	10	105	36	0.063	Electrolyte: 0.1 M $HClO_4$; Scan rate: 2 mV s^{-1}	3
Commercial WC	10	~300 (a)	73	0.018	Electrolyte: 1 M H_2SO_4; Scan rate: 5 mV s^{-1}	1
$W_{0.5}$Ani/GnP	10	120	68.6 (b)	0.038	Electrolyte: 0.1 M $HClO_4$; Scan rate: 2 mV s^{-1}	4

W_2C/GnP	10	186	64.7 (b)	0.024	Electrolyte: 0.1 M $HClO_4$; Scan rate: 2 mV s^{-1}	4
WC	20	444	—	—	Electrolyte: 0.1 M H_2SO_4; Scan rate: 5 mV s^{-1}	5
Fe-WCN	10	220	47.1	—	Electrolyte: H_2SO_4 (pH=1); Scan rate: 5 mV s^{-1}	6
Carbon coated cobalt–tungsten carbide Co_6W_6C	10	200	75	0.0286	Electrolyte: 0.5 M H_2SO_4; Scan rate: 50 mV s^{-1}	7
Porous WC thin film	10	274	67	—	Electrolyte: 0.5 M H_2SO_4; Scan rate: 5 mV s^{-1}	8
CNS@WC/GF	10	65	61	0.0758	Electrolyte: 1 M H_2SO_4; Scan rate: 2 mV s^{-1}	9
$Fe_xCo_{1-x}P$/CC	10	37	30	—	Electrolyte: 0.5 M H_2SO_4; Scan rate: 2 mV s^{-1}	15
WP_2	10	54	57	0.017	Electrolyte: 0.5 M H_2SO_4; Scan rate: 2 mV s^{-1}	16
CoP/CC	10	67	51	0.288	Electrolyte: 0.5 M H_2SO_4; Scan rate: 2 mV s^{-1}	17

(a) The overpotential (η_{10}) was estimated from *JV* polarization curves.

(b) The Tafel slope was obtained from plots of E vs. $\log(R\text{ct})^{-1}$.
(c) The exchange current density was estimated from Tafel plots.

Table S2. Comparison of HER performance for **P-W_2C@NC** with other tungsten carbide-based electrocatalysts in basic media.

Catalysts	Onset Potential (mV)	Current density (j, mA cm^{-2})	η at corresponding j (mV)	Tafel slope (mV $decade^{-1}$)	Experimental conditions	Ref.
P-W_2C@NC	**26**	**10** **50**	**63** **110**	**65**	Electrolyte: 1 M KOH; Scan rate: 2 mV s^{-1}	**This work**
WC-CNTs	16	10 33.1	137 300	106	Electrolyte: 0.1 M KOH; Scan rate: 50 mV s^{-1}	2
Fe-WCN	120	10	250	47.1	Electrolyte: alkaline medium (pH: 13); Scan rate: 5 mV s^{-1}	6
Carbon coated cobalt–tungsten carbide Co_6W_6C	—	10	73	25	Electrolyte: 1 M KOH; Scan rate: 50 mV s^{-1}	7
CNS@WC/GF	—	10	68	72	Electrolyte: 1 M KOH; Scan rate: 2 mV s^{-1}	9
WN/CC	—	2	143	—	Electrolyte: 1 M KOH; Scan rate: 2 mV s^{-1}	18
Fe-CoP/Ti		10	78	75	Electrolyte: 1 M KOH; Scan rate: 2 mV s^{-1}	20
Ni_2P/CC	74	10	102	65	Electrolyte: 1 M KOH; Scan rate: 2 mV s^{-1}	21

Table S3. Comparison of HER performance for **P-W_2C@NC** with other precious-metal-free electrocatalysts in neutral media.

Catalysts	Current density (j, mA cm^{-2})	η at corresponding j (mV)	Experimental conditions	Ref.
P-W_2C@NC	**10**	**185**	Electrolyte: 1 M phosphate buffer (pH=7); Scan rate: 2 mV s^{-1}	**This work**
Carbon coated cobalt–tungsten carbide Co_6W_6C	10	224	Electrolyte: 0.1 M phosphate buffer (pH=7); Scan rate: 50 mV s^{-1}	7
WC	8.8	300	Electrolyte:sodium-phosphate-buffer(pH=7);	10
$CuMoS_4$	2	210	Electrolyte: 0.1 M phosphate buffer (pH=7); Scan rate: 10 mV s^{-1}	11
Co-NRCNTs	10	540	Electrolyte: 0.1 M phosphate buffer (pH=7); Scan rate: 50 mV s^{-1}	12
FeP nanoparticles	10	102	Electrolyte: 1 M phosphate buffer (pH=7); Scan rate: 1 mV s^{-1}	13
Mo_2C@NC	10	156	Electrolyte: 0.1 M phosphate buffer (pH=7); Scan rate: 50 mV s^{-1}	14

WP_2	Onset overpotentia	60	1.0 M phosphate buffer (pH=7)	16
CoP/CC	Onset overpotentia	45	1.0 M phosphate buffer (pH=7)	17
WN/CC	2	186	1.0 M phosphate buffer (pH=7)	18
WP/CC	Onset overpotentia	100	1.0 M phosphate buffer (pH=7)	19

[1] D. J. Ham, R. Ganesan and J. S. Lee, *Int. J. Hydrogen Energy*, 2008, **33**, 6865–6872.

[2] X .J. Fan, H. Q. Zhou, X. Guo, ACS Nano 2015, 9, 5125-5134

[3] F. K. Meng, E. Y. Hu, L. H. Zhang, K. Sasaki, J. T. Muckerman and E. Fujita, *J. Mater. Chem. A,* 2015, 3,18572

[4] W. F. Chen, M. S. Schneider, K. Sasaki, C. H. Wang, J. Schneider, S. Iyer, S. Iyer, Y. Zhu, J. T. Mucherman and E. Fujita, *ChemSusChem*, 2014, **7**, 2414–2418.

[5] S. Wirth, F. Harnisch, M. Weinmann, U. Schröder, *Appl. Catal. B*, 2012, 126, 225– 230

[6] Y. Zhao, K. Kamiya, K. Hashimoto, S. Nakanishi, *Angew. Chem. Int. Ed*.2013, 52, 13638–13641.

[7] Y. P. Liu, G.-D. Li, L. Yuan, L. Ge, H. Ding, D. J. Wang and X. X. Zou, Nanoscale 2015, 7, 3130–3136

[8] H. L. Fei, Y. Yang, X. J. Fan, G. Wang, G. D. Ruan and J. M. Tour, J. Mater. Chem. A, 2015, 3, 5798

[9] Y. Shen, L. Li, J. Y. Xi and X. P. Qiu, *J. Mater. Chem. A*, 2016, 4, 5817-5822.

[10] F. Harnisch, G. Sievers and U. SchrÖder., *Appl. Catal. B*, 2009, 89, 455-458.

[11] P. D. Tran, M. Nguyen, S. S. Pramana, A. Bhattacharjee, S. Y. Chiam, J. Fize, M. J. Field, V. Artero, L. H. Wong, J. Loo and J. Barber., *Energy Environ. Sci.* 2012, *5*, 8912.

[12] X. X. Zou, X. X. Huang, A. Goswami, R. Silva, B. R. Sathe, E. Mikmeková, and T. Asefa., *Angew. Chem. Int. Ed.* 2014, *53*, 4372.

[13] J. F. Callejas, J. M. McEnaney, C. G. Read, J. C. Crompton, A. J. Biacchi, E. J. Popczun, T. R. Gordon, N. S. Lewis, and R. E. Schaak., *ACS NANO*, 2014,8, 11101.

[14] Y. P. Liu, G. T. Yu, G. D. Li, Y. H. Sun, T. Asefa, W. Chen, and X. X. Zou., *Angew. Chem. Int. Ed*. 2015, 54, 10752-10757.

[15] C.Tang, L. F. Gan. R.Zhang, W. B. Lu, . Jing, A. M. Asiri, X. P. Sun, J. Wang, L.

Chen, Nano Lett, DOI: 10.1021/acs.nanolett.6b03332

[16] Z. C. Xing, Q. Liu, A. M. Asiri, X. P. Sun, ACS Catal. 2015, 5, 145−149.

[17] J. Q. Tian, Q.Liu, A. M. Asiri, X. P. Sun, J. Am. Chem. Soc. 2014, 136, 7587−7590

[18] J. L. Shi, Z. H. Pu, Q. Liu, A. M. Asiri, J. M. Hua, X. P. Sun, Electrochimica Acta 154 (2015) 345–351

[19] Z. H. Pu, Q. Liu, A. M. Asiri, X. P. Sun, ACS Appl. Mater. Interfacesdx. doi.org/10.1021/am5060178

[20] C. Tang, R. Zhang, W. B. Lu, L. B.He, X.Jiang, A. M. Asiri, X. P. Sun, *Adv. Mater.* 2016

[21] P. Jiang, Q. Liu, X. P. Sun, Nanoscale, 2014, 6, 13440

4.Theoretical calculation method.

4.1 Computational Methods and Models

Our calculations were performed using Vienna ab initio simulation package (VASP).[1,2] All DFT calculations were treated within the generalized gradient approximation (GGA) with the PBE functional for the exchange and correlation effects of the electrons.[3] A cutoff energy of 350-eV for the grid integration was utilized and the convergence threshold for force and energy was set as 0.04 eV/Å and 10^{-4} eV, respectively. Ion cores are described by projector augmented wave PAW potentials.[4,5] Monkhorst-Pack grids of 3 × 3 × 1 k points were used for all calculations. For geometry optimization, the top three layers of W_2C (121) and graphene were allowed to relax, while the rest of W_2C (121) (the bottom three layers) remained fixed.

4.2 The calculation of free energies

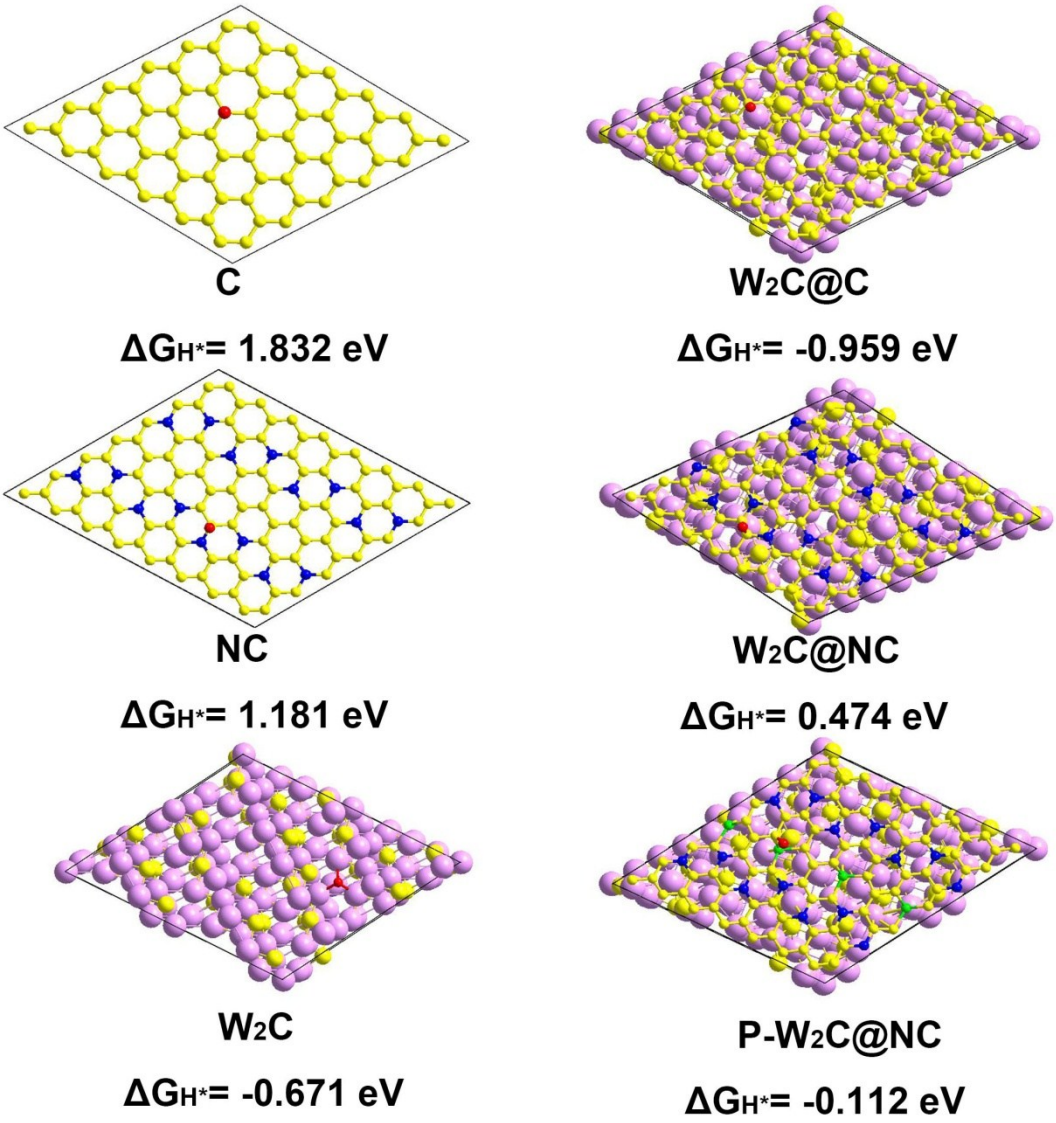

Figure S11. The theoretical models of H adsorbed on: (a) W_2C, (b) C, (c) W_2C@C, (d) NC, (e) W_2C@NC and (f) P-W_2C@NC. The yellow, blue, pink, green and red balls represent C, N, W, P and H atoms, respectively.

The theoretical models of the studied systems are shown in Figure S9, and the corresponding lattice parameters used in our calculations have been presented in Table S4. W_2C (121) surface is modeled. To compare the catalytic activity of different studied systems, the free energies of the intermediates were evaluated by the equation $\Delta G(H^*) = \Delta E(H^*) + \Delta ZPE - T\Delta S$, where H* denotes a H atom adsorbed on the surface and $\Delta E(H^*)$, ΔZPE and ΔS denote the binding energy, zero point energy change and entropy change between the H* and the gas phase, respectively. Therefore, the equation $\Delta ZPE = ZPE(H^*) - 1/2ZPE(H_2)$ can be used to estimate ΔZPE for H*. The gas phase entropy of H was taken from ref. [6]. According to the analysis of Bader charge[7] of atoms on the surfaces, we selected several adsorption sites on each surface to investigate the capacity of H adsorption on different surfaces. The most active site of H adsorption on each surface was showed in Figure S1. The obtained binding energies, zero point energies and the free energies for H adsorption on different surfaces are listed in Table S5. It will be an excellent catalyst for HER if $\Delta G(H^*) \approx 0$.

Table S4. The lattice parameters (Å) of the supercells for all the systems.

Models	a	b	c
C	14.76	14.76	18.00
CN	17.08	19.54	18.00
W_2C	16.07	18.30	18.00
W_2C@C	16.46	17.78	18.00
W_2C@NC	16.41	17.71	18.00
P-W_2C@NC	16.50	17.76	18.00

Table S5. The $\Delta E(H^*)$, $ZPE(H^*)$ and $\Delta G(H^*)$ values of the H* adsorbed on different surfaces.

Models	$\Delta E(H^*)$/eV	$ZPE(H^*)$/eV	$\Delta G(H^*)$/eV
C	1.483	0.301	1.832
CN	0.821	0.289	1.181
W_2C	-0.930	0.187	-0.671
W_2C@C	0.592	0.296	0.959
W_2C@NC	0.083	0.319	0.474
P-W_2C@NC	-0.497	0.313	-0.112

[1] G. Kresse, J. Hafner, *Phys. Rev. B* 1993, *47*, 558.
[2] G. Kresse, J. Hafner, *Phys. Rev. B* 1994, *49*, 14251.
[3] J. P. Perdew, K. Burke, M. Ernzerhof, *Phys. Rev. Lett*. 1996, *77*, 3865.
[4] P. E. Blochl, *Phys. Rev. B* 1994, *50*, 17953.
[5] G. Kresse, D. Joubert, *Phys. Rev. B* 1999, *59*, 1758.
[6] Y. P Liu, G. T. Yu, G. D. Li, Y. H. Sun, T. Asefa, W. Chen, X. X Zou, *Angew. Chem. Int. Ed*. 2015, *54*, 10752.
[7] G. Henkelman, A. Arnaldsson, H. Jónsson, *Comput. Mater. Sci*. 2006, *36*, 254.

atom	original sample (atom%)	acid etching (atom%)
C	69.69	90.1
N	7.61	7.02
P	2.73	0.15
W	19.97	2.73

Table S6. Comparison of atom percentage of P-W_2C@NC before and after acid etching.

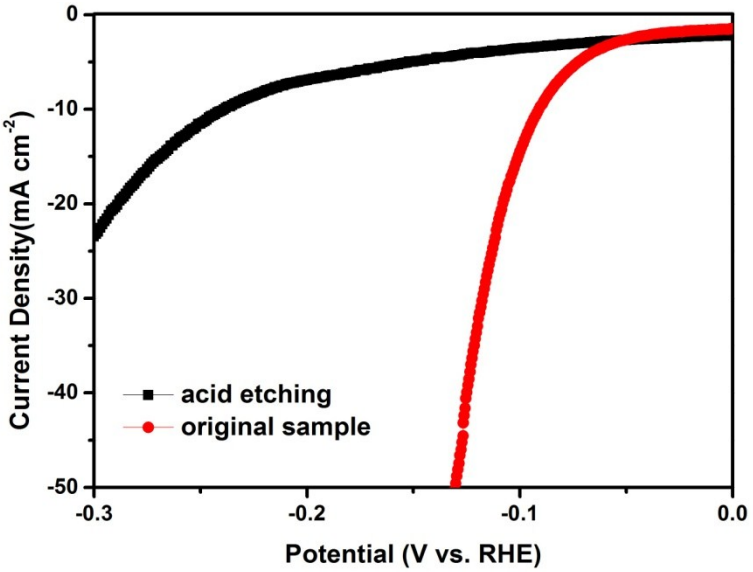

Figure S12. Comparison of polarization curves of P-W_2C@NC before and after acid etching.